Solid Earth Discuss., https://doi.org/10.5194/se-2019-3
Manuscript under review for journal Solid Earth
Discussion started: 14 January 2019

Topographic changes due to the 2004 Chuetsu thrusting earthquake in low mountain region

Zhikun Ren[1,2], Takashi Oguchi[3], Peizhen Zhang[2], Shoichiro Uchiyama[4]

1 Key Laboratory of Active Tectonics and Volcanos, Institute of Geology, China Earthquake Administration, P.O. Box 9803, Beijing 100029, China; rzk@ies.ac.cn

[2]State Key Laboratory of Earthquake Dynamics, Institute of Geology, China Earthquake Administration, P.O. Box 9803, Beijing 100029, China

[3]Center for Space Information Science, The University of Tokyo, Chiba, 2778568 Japan

[4]National Research Institute of Earth Science and Disaster Prevention, Tsukuba, Ibaraki,3050006 Japan

*Corresponding address:

State Key Laboratory of Earthquake Dynamics

Institute of Geology

China Earthquake Administration

Beijing 100029, China

Email:**rzk@ies.ac.cn**

lzkren@gmail.com

Solid Earth Discuss., https://doi.org/10.5194/se-2019-3
Manuscript under review for journal Solid Earth
Discussion started: 14 January 2019

Abstract

The co-seismic landslide volume information is critical to understanding the role of strong earthquake in topographic evolution. However, the co-seismic landslide volumes are mainly obtained using statistical scaling laws, which are not accurate enough for quantitative studies of the spatial pattern of co-seismically induced erosion and the topographic changes caused by the earthquakes. The availability of both pre- and post- earthquake high-resolution DEMs provide us the opportunity to try new approach to get robust landslide volume information. Here, we propose a new method in landslide volume estimate and tested it in Chuetsu region, where a Mw 6.6 earthquake occurred in 2004. Firstly, we align the DEMs by reconstructing the horizontal difference, then we quantitatively obtained the landslide volume in the epicentral area by differencing the pre- and post-earthquake DEMs. We convert the landslide volume into the distribution of average catchment-scale seismically induced denudation. Our results indicate the preserved topography is not only due to the uplifting caused by fault-related folding on the hangwall of Muikamachi fault, but also undergone erosion caused by the seismically induced landslides. Our findings reveal that Chuetsu earthquake mainly roughens the topography in the Chuetsu region of low elevation. This study also reveal that the differential DEM method is a valuable approach in analyzing landslide volume, as well as quantitative geomorphic analysis.

Keywords: Chuetsu earthquake; topographic change; LiDAR; Differential DEM; denudation

1. Introduction

It is increasingly recognized that the role of tectonic events is critical to understanding topographic evolution, such as strong earthquakes. Strike-slip earthquakes mainly cause horizontal deformation, normal fault earthquakes mainly occurred in extensional environment than reduce the topography, and thrust earthquake is the main one causing surface uplift, hence mountain building. It has been realized that strong thrust earthquakes play important role in the topographic evolution in regions of steep relief and high elevation, such as the marginal zones of high plateau at Himalaya (Avouac, 2003; Larsen and Montgomery, 2012; Morell et al., 2015; Owen, 2010), Longmen Shan (Hovius et al., 2011; Li et al., 2014; Parker et al., 2011; Ren et al., 2014a) and Andes (McPhillips et al., 2014). Previous studies demonstrated that the landslides are thought to limit the slope (Blöthe et al., 2015; Burbank et al., 1996) and height of mountain peaks above adjacent river valleys in steep orogenic regions (Larsen and Montgomery, 2012; McPhillips et al., 2014; Roering, 2012). Recent studies found that the erosion caused by landslides did not change much in response to climatic changes; hence, the tectonic events such as earthquakes are the primary landslide trigger in the arid foothills of Peru in steep Andes (McPhillips et al., 2014). Quantifying erosion rate is critical to understanding the role of tectonic events in mountain building. However, due to the long-term mountain building and topographic evolution, previous studies are mainly regional studies based on sparse thermochronological dating (Kirby et al., 2002; Wang et al., 2012), cosmogenic dating (Ansberque et al., 2015; Godard et al., 2010; Ouimet, 2010) or modern hydrological observations (Dadson et al., 2003) in region of high mountain area. These

Solid Earth Discuss., https://doi.org/10.5194/se-2019-3
Manuscript under review for journal Solid Earth
Discussion started: 14 January 2019

regional studies could not show the details of how tectonic events act in topographic evolution of low mountain region. Strong earthquakes are the most recent tectonic events, which provide us the valuable opportunity to study the role of such events in current topographic evolution of low mountain region. However, the co-seismic landslide volumes are usually obtained using statistical scaling laws, which has large uncertainties in different regions by applying same scaling laws. Different researchers could get totally different co-seismic landslide volumes for one earthquake using different methods (Li et al., 2014; Marc et al., 2015; Parker et al., 2011; Ren et al., 2014b; Ren et al., 2017).

Recently, the high-resolution and multi-temporal Light Detection and Ranging (LiDAR) Digital Elevation Models (DEMs) or DEM generated from stereo pair of remote sensing images have been proven valuable in monitoring geomorphic, co-seismic and volcanic surficial deformations (Cowgill et al., 2012; Lane et al., 2001; Ren et al., 2014a; Stumpf et al., 2014; Wheaton et al., 2010; Zhou et al., 2015; Zielke et al., 2010). By differential pre- and post-earthquake DEM, we could quantitatively analysis the topographic changes and evaluate the landslide volume. It has been used to derive co-seismic landslide volumes in Longmen Shan region by differencing pre- and post- Wenchuan earthquake DEMs, as well as topographic analysis (Ren et al., 2014a). However, in region of low mountain, the role of strong earthquakes in topographic evolution is rarely reported. The 2004 Mw 6.6 Chuetsu earthquake occurred in Niigata prefecture in Japan, where the local relief of the epicentral area is low with maximum elevation of 765 m (Fig. 1). In this study, we use the high-resolution pre- and

Solid Earth Discuss., https://doi.org/10.5194/se-2019-3
Manuscript under review for journal Solid Earth
Discussion started: 14 January 2019

post-earthquake DEM (GSI, 2007) to study the topographic changes due to the Chuetsu earthquake, by comparing the slope angle, slope aspect, relief and roughness pre- and post-earthquake. The co-seismic denudation distribution pattern was also analyzed using the co-seismic landslide volume with the availability of multi-temporal high-resolution topographic data. We finally discussed the role of earthquake in topographic evolution at Chuetsu area of low mountain.

2. Tectonic Setting

The 2004 Mw 6.6 Chuetsu earthquake occurred at Chuetsu, Niigata prefecture Japan, where the convergent plate boundary between the Amurian and Okhotsk plates is located (Fig. 1, (Okamura et al., 2007; Okamura et al., 1995; Wei and Seno, 1998)). The epicentral area is of low elevation with maximum of 765 m, which is composed of sedimentary and volcanic rocks from Holocene to Miocene. The sediments were mainly formed in the early Miocene, concurrently with the opening of the Japan Sea (Fig. 1). The sediments have been folded under E-W to WNW-ESE compressional stress field since ~2-3 Ma (e.g., (Hirata et al., 2005; Okamura, 2003)). The continued compression deformed the strata, landforms and caused the repeated seismicities in Chuetsu area. The Shinano River is the main river flow through the Chuetsu area where the flood plain is mainly composed of Holocene to Late Pleistocene sediments (Fig. 2). The mountain area is mainly composed of Pleistocene to Pliocene sediments, accompanied with a tectonic window composed of Jurassic sediments (Fig. 2). The uplifting of the mountain is proposed to be due to fault-related folding caused by the thrust along the NS trending

Muikamachi-Bonchi-Seien fault (Fig. 2,)(Kato et al., 2005; Kato et al., 2006; Okamura et al., 2007). The 2004 Chuetsu earthquake is a thrust-dominated earthquake with minor lateral motion (Maruyama et al., 2005). It has been reported that there is a co-seismic surface rupture zone of 1 km in length, with ~20 cm vertical co-seismic offset and lateral offset less than 20 cm on a previously unmapped fault (Maruyama et al., 2005), which lies along the northward extending of the Muikamachi fault (Fig.2 , (Nakata and Imaizumi, 2002; RGAFJ, 1991)). Hence, the most possible causative fault of the Chuetsu earthquake is the Muikamachi fault, according to the focal mechanism and location of surface ruptures (Maruyama et al., 2005). Previous studies mapped the subsurface fault with detachment in depth of ~10-13 km, which agreed well with the distribution of aftershocks (Kato et al., 2005; Kato et al., 2006; Okamura et al., 2007). They found that the fault-related folding on the hanging wall of the Muikamachi fault was responsible for the growth of the geological structures (Kato et al., 2005; Kato et al., 2006; Okamura et al., 2007; Suppe, 1983). Paleoseismology studies reveal at least two strong earthquakes occurred in the past 9000 years prior to the occurrence of the 2004 Chuetsu earthquake(Maruyama et al., 2005). The co-seismic displacements of the two paleoearthquakes were almost identical at ~1.5 m, which was almost 15 times of the 2004 event (~10 cm). The 2004 Chuetsu earthquake triggered thousands of co-seismic landslides, which dramatically modified the local topography (Chigira and Yagi, 2006; Dou et al., 2015; Sato et al., 2005; Wang et al., 2007). Hence, the mountain growth in the epicentral area should be closely related to the co-seismic landslides caused by repeated strong earthquakes.

3. Data and Methods

3.1. Data

The pre-earthquake DEM is of 10 m in resolution with absolute vertical precision within 2.5 meter. The 10-m-resolution DEM is generated from stereo pairs of aerial photographs or topographic maps that covering the whole Japan area at Geospatial Information Authority (GSI) of Japan (Freely available at http://fgd.gsi.go.jp/download). The post-earthquake DEM is of 2 m resolution with root-mean-square (RMS) error within 0.12 m that generated from airborne LiDAR data surveyed in 2005 with point density larger than 1 pt/m^2, released by the GSI of Japan ((GSI, 2007). These DEMs are of higher precision than that used in our previous studies in Wenchuan area (Ren et al., 2014b) (Fig. 3). The landslide inventory map is interpreted based on high-resolution aerial photograph, by the National Research Institute for Earth Science and Disaster Prevention (NIED), Japan (Fig. 4, (Chigira and Yagi, 2006; Dou et al., 2015; Sato et al., 2005; Wang et al., 2007)). The geological information is derived from the 1:200,000 geological maps provided by the Geological Survey of Japan (GSJ) (Figs. 2 and 4a, Freely available at https://gbank.gsj.jp/seamless/index_en.html) and the active fault map of Japan (Fig. 1; (Nakata and Imaizumi, 2002; RGAFJ, 1991)).

3.2. Methods

3.2.1. Differential DEM

With the availability of high-resolution DEM data pre- and post-earthquake, especially the LiDAR DEM, the differential DEM method are widely used in detecting topographic changes (Chen et al., 2006; Ren et al., 2014a; Stumpf et al., 2014), co-seismic deformations (Cowgill et al., 2012; Nissen et al., 2014; Zhou et al., 2015) as well as sediment budgets (Lane et al., 2001; Wheaton et al., 2010) . Previous studies have shown that the differential DEM method using multiple-scale and multiple-source DEMs is effective in detecting topographic changes caused by co-seismic landslides (Chen et al., 2006; Ren et al., 2014a; Ren et al., 2017). The available of the pre- and post-earthquake DEMs in Chuetsu area provide us the opportunity to study the topographic changes caused by the co-seismic landslides due to the 2004 Chuetsu earthquake. In differential DEM method, the precise georeference and correlation between the multi-temporal DEMs is one of the key issues before subtracting. To analysis the topographic changes under compression environment, we are mainly interest of the vertical deformations. The horizontal differences between the pre-and post-earthquake DEMs were calculated and then reconstructed by back-slipping the horizontal differences. The cosi-corr software is developed to measure sub-pixel ground deformation using optical satellite and aerial images, which has an accuracy of 1/10 of the input pixel size (Ayoub et al., 2015; Hollingsworth et al., 2012; Leprince et al., 2007; Zhou et al., 2015). In this study, we could estimate the horizontal differences between the pre- and post-earthquake DEMs using the cosi-corr software (freely available at www.tectonics.caltech.edu/slip_history/spot_coseis/index.html), following Zhou et al.'s method (Zhou et al., 2015). The airborne LiDAR DEM was downsampled to 10 m to match the pre-earthquake DEM. We used a correlation window of 64 pixels followed by 32 pixels with a step of 4 pixels (40 m). The sub-pixel matching procedure was performed on the frequency content, which is more accurate than the statistical correlator (Ayoub et al., 2015; Zhou et al., 2015). Consequently, we got the NS (Fig. 3a) and EW (Fig. 3b) components of the horizontal differences between the pre- and post-earthquake DEMs (Fig. 3). Then by reconstructing the mean horizontal differences in both directions to the whole DEM, we obtained the precisely geo-referenced and correlated DEMs. Finally, by differencing the pre- and post-earthquake DEMs, we obtained the vertical deformations caused by the Chuetsu earthquake (Figs. 3c and 4). The largest landslide clearly shows the source and deposit areas, which occurred in the low mountain composed of late Miocene to Pliocene non-marine sediments (Fig. 4). Meanwhile, the derived landslide volumes also show consistent results that deep-seated landslides are the main contributor to the landslide volumes (Fig. 5).

3.2.2. Topographic Analyses

Steep slopes are prone to landslides (Burbank et al., 1996; Dai and Lee, 2002; Densmore et al., 1998), such as the co-seismic landslides triggered by the 2008 Wenchuan Mw 7.9 earthquake which mainly

Solid Earth Discuss., https://doi.org/10.5194/se-2019-3
Manuscript under review for journal Solid Earth
Discussion started: 14 January 2019

occurred on slopes with angles larger than 30° (Ren and Lin, 2010). Previous studies have found that slope angle, slope aspect, relief and roughness are the four main topographic features widely used in geomorphological studies, which could be used to analysis the topographic changes due to the co-seismic landsliding. Statistical comparison of the pre- and post-earthquake topographic features has been proven to be useful in analyzing the co-seismic topographic changes (Ren et al., 2014a). In this study, based on the downsampled 10 m resolution pre- and post-earthquake DEMs, we compare the pre- and post-earthquake slope angle, slope aspect, relief and roughness, respectively (Fig. 6). The co-seismic displacement is less than 20 cm in the epicentral area, hence, the topographic changes are mainly due to co-seismic landsliding. Thus, in this study, we statistically compare the topographic changes within each landslide polygon (Fig. 6).

3.2.3. Catchment-scale Denudation depth

Landsliding is the dominant mass wasting process in humid uplands (Hovius et al., 1997), thus, it is reasonable to derive the denudation using the landslide volumes. The topographic changes within the landslide area should be much larger than the ~10 cm co-seismic displacements. Thus it is reliable to derive landslide volume using the subtracted DEM. We calculated the co-seismic landslide volumes in the epicentral area, by summing the elevation changes within the landslide area and multiplying the summed value by the area of one pixel (100 m^2). There are positive values and negative values for each

Solid Earth Discuss., https://doi.org/10.5194/se-2019-3
Manuscript under review for journal Solid Earth
Discussion started: 14 January 2019

single landslide, because there are source and deposit areas, correspondingly (Fig. 4b and 4c). Hence we firstly sum both the positive and negative value for each landslide, then summed the absolute value together and finally take the average value as the landslide volume for this landslides. The catchments are derived using the flow accumulation data of the streams and outlet data of each catchment from the pre-earthquake DEM with stream length as short as 5 km (Fig. 7). To obtain distribution pattern of the catchment-scale denudation depth, we summed the landslide volumes within each catchment. The average denudation depth was obtained by dividing the summed landslide volume by the catchment area (Figs. 7-8).

4. Results

Using cosi-corr software, we obtained the NS component difference of -0.27 m with standard deviation (STD) of 3.12 m and the EW component difference of 0.21 m with STD of 3.37 m (Figs. 3b and c). Before differential the DEMs, we first reconstruct the corresponding differences of NS and EW components. Then we obtain the elevation changes by subtracting the pre-earthquake DEM from the post-earthquake DEM. The flat ground surfaces that located far from the epicentral area should be stable during the earthquake, i.e., the real elevation changes should be nearly zero. Hence, the obtained elevation differences at such regions represent the accuracy of the differential DEM in this study. The elevation differences ranges from -0.46 m to 0.32 m at the non-deformed flat region shown in figure 3c

(Fig. 3c). We then obtain the mean elevation change of the whole region of -0.24 m with STD of 2.22 m (Figs. 3d) by eliminating the elevation changes between -0.46 m and 0.32 m, i.e., setting the delta-z values within this range to 0. The obtained mean vertical deformation is comparable with the maximum co-seismic displacement from Interferometric Synthetic Aperture Radar (InSAR) results (Ozawa et al., 2005) and field investigations (Maruyama et al., 2005). In the landslide region, the elevation changes could reach tens of meter, which are much greater than 0.32 m and less than -0.46 m, hence it is reliable to analyze the topographic changes using the pre- and post- earthquake DEMs. The mean elevation change in the landslide region is 0.08 with STD of 2.17 m (Fig. 4b). As shown in Figure 4c, the landslide scarp and toe of the largest landslide is clearly shown on the differential DEM map. The results show the total volume of the 330 deep-seated landslides is ~0.26 km^3 (Fig. 5), which is comparable with the total volume of ~0.30 km^3 of the ~6000 shallow landslides (Fig. 5). The catchment-scale average denudation depth distribution shows maximum denudation of 894 mm, which did not locate right above the surface ruptures (Figs. 7-8, (Maruyama et al., 2005)). The maximum denudation correlates with the uplifting pattern in the epicentral area suggested by the fault-related folding on the hangwall of the Muikamachi fault (Fig. 8, (Kato et al., 2005; Kato et al., 2006; Okamura et al., 2007)).

The co-seismic topographic changes in the epicentral area show consistent increase in slope angle, relief

Solid Earth Discuss., https://doi.org/10.5194/se-2019-3
Manuscript under review for journal Solid Earth
Discussion started: 14 January 2019

and roughness (Fig .6). The comparison of the pre- and post-earthquake topographic features within each catchment also indicate the average hillslope, relief and roughness are all increased after the Chuetsu earthquake (Fig .6). The slope aspect decreases in 0°-135° and 270°-360° and increases in 135°-270° (Fig. 6). The observed slope aspect changes might be related with the co-seismic lateral displacement of the 2004 Chuetsu earthquake, which was reported to be ~10-20 cm (Maruyama et al., 2005).

5. Discussion

The occurrence of the Chuetsu earthquake provides a valuable opportunity to quantitatively analysis the co-seismic topographic changes and denudation caused by co-seismic landslides with the availability of the pre- and post- earthquake DEM in the epicentral region, hence discussing the tectonic process and topographic growth in region of low mountain. This study might be the first time to study the topographic changes using differential DEM method in region of low mountain. The key question in differential DEM study is the pre- and post- earthquake DEMs are of different sources, which might represent different surfaces, such as the topographic or bare-earth surface. Usually, the DEM from stereo pair of images should represent the topographic surfaces including the canopy of the forest, and the LiDAR derived DEM represents the bare-earth DEM. However, in this study, there are no systematical elevation errors observed. Meanwhile, the blank area in Fig 4b show the elevation differences beyond -0.46 m to 0.32 m. The canopy of forest could not be such small. Hence, the differential DEM results should represent the canopy of the forest, which indicate that the pre- and post-earthquake DEMs are referring the same surface, i.e., our results represent the real co-seismic elevation differences, however, due to the precision and resolution of the DEMs, it could not show the co-seismic vertical deformations less than ~20 cm clearly. In this study, based on the pre- and post-earthquake DEMs, we statistically analyzed the topographic changes caused by the Chuetsu earthquake in terms of the slope angle (Fig. 7a), slope aspect (Fig. 7b), relief (Fig. 7c), roughness (Fig. 7d) and the catchment-scale denudation (Figs. 7-8). The slope angle, relief and roughness are all coseismically increased after the Chuetsu earthquake in landslide-scale (Fig. 6) and catchment-scale (Figs. 8a-c) at the epicentral area (Fig. 6). The slope aspect changes show decrease in 0°-135° and 270°-360° and increase in 135°-270°, which might be associated with the co-seismic lateral displacement along the NS trending rupture (Maruyama et al., 2005). The comparisons of pre- and post-earthquake data suggest the Chuetsu earthquake is mainly roughening the topographic relief (Fig. 6), which is consistent with the role of long-term seismic landsliding (Blöthe et al., 2015; Larsen and Montgomery, 2012; McPhillips et al., 2014; Roering, 2012).

In this paper, the co-seismic landslide volumes are obtained using differential DEM method, then we convert the landslide volume information into seismically induced erosion. We find that, in the Chuetsu area, the catchment-scale denudation depth distribution did not show direct correlation with the distance to the surface rupture (Fig. 8). The denudation distribution pattern shows correlation with the uplifting pattern suggested by fault-related folding on the hangwall of the Muikamachi Fault (Fig. 8, (Okamura et al., 2007)). The fault-related folding suggest the main uplifting area lies ~8-10 km away from the Mukamachi fault on the hangwall (Kato et al., 2005; Kato et al., 2006; Okamura et al., 2007; Suppe, 1983). However, in the steep Wenchuan area, previous studies have found that long-term high denudations are concentrated in a narrow zone along the Longmen Shan Thrust Belt, revealed by erosion rates from kyr-scale cosmogenic ^{10}Be and Myr-scale low temperature thermochronology dating methods (Godard et al., 2010; Kirby et al., 2002; Ouimet, 2010). The highest co-seismic denudation also mainly concentrated in the narrow corridor between the co-seismic surface ruptures produced by the 2008 Wenchuan earthquake (Ren et al., 2014a). Hence there might be two possibilities why the topographic relief profile did not directly correlate with the uplifting pattern in Chuetsu region (Fig. 8). The first possible reason might be due to the erosion differences. The high erosion occurred in the high uplifting area due to fault-related folding; but the area near the fault is of low erosion and uplift (Fig. 8). Thus, the almost homogeneous topographic relief is preserved in the epicentral area under the coupling process of co-seismic uplift and denudation. The correlation between the denudation and uplifting also indicates the topographic growth in orogenic belt is closely related with the deformations associated with the major faults, especially in regions that the uplifting is dominated by fault-related folding (Okamura et al., 2007; Suppe, 1983). Hence, the strong earthquakes should play important role in the mountain growth in the epicentral area since initiation of compression and folding at ~2-3 Ma (Hirata et al., 2005; Okamura, 2003). The second possible reason is that the topography near the Muikamachi fault might be due to the strong paleoearthquakes associated with large co-seismic vertical offsets as that revealed by trenching (Maruyama et al., 2007). Paleoseismological studies reveal at least two strong earthquakes occurred during the past ~9000 years, which produced co-seismic vertical displacement that are almost 15 times of that produced by the Chuetsu earthquake (Maruyama et al., 2005; Maruyama et al., 2007). A vertical slip rate of 0.4 mm/yr was calculated using the dating results of the displaced units in the trench (Maruyama et al., 2007). The Chuetsu area is composed of young sediments mainly formed since Miocene, which is under continued thrusting and folding since ~2-3 Ma (Hirata et al., 2005; Okamura, 2003). The total uplifting could be roughly estimated to be ~800-1200 m, which is consistence with current mountain height of ~700-800 m considering that there is also erosion caused by landslides.

6 Conclusions

Here, we report the role of a Mw 6.6 Chuetsu earthquake in the topographic evolution of the young and low mountain region, by quantitatively comparing the pre- and post- earthquake high-resolution DEMs. Our results show, after the Chuetsu earthquake, the slope angle, relief and roughness are coseismically increased at the epicentral area; which is different with that occurred in the old and steep Longmen Shan

Solid Earth Discuss., https://doi.org/10.5194/se-2019-3
Manuscript under review for journal Solid Earth
Discussion started: 14 January 2019

orogenic region. The co-seismically induced landslides play important role in balancing the long-term uplift by concentrated high denudation at the uplifted area far from the surface fault traces, while according to the 2008 Wenchuan earthquake, the co-seismic denudation show different pattern that concentrated right at the surface rupture zones. The preserved mountain peaks are not only uplifted by thrusting and folding but also undergone erosion caused by seismically induced landslides. Finally, we suggest that the strong earthquakes might play different roles in topographic evolutions in low and steep mountain regions. The findings also reveal that the differential DEM method is a powerful and robust approach in evaluating co-seismic landslide volumes as well as quantitative geomorphic analyses.

Acknowledgements

We appreciate Dr. Zhou Yu for his help in processing the DEM data and valuable suggestions. The authors want to thank Geospatial Information Authority (GSI) of Japan, National Research Institute for Earth Science and Disaster Prevention (NIED), Japan and Geological Survey of Japan (GSJ) for sharing the topographic, landslide inventory and geological data. This work was funded by the National Key Research and Development Program of China (2017YFC1500401), State Key Laboratory of Earthquake Dynamics (LED2014A03) and National Natural Science Foundation of China (41472201, 41761144071).

Solid Earth Discuss., https://doi.org/10.5194/se-2019-3
Manuscript under review for journal Solid Earth
Discussion started: 14 January 2019

References

Ansberque, C., Godard, V., Bellier, O., De Sigoyer, J., Liu-Zeng, J., Xu, X., Ren, Z., Li, Y., and Team, A. S. T. E. R.: Denudation pattern across the Longriba fault system and implications for the geomorphological evolution of the eastern Tibetan margin, Geomorphology, 246, 542-557, 2015.

Avouac, J.-P.: Mountain building, Erosion, and the seismic cycle in the Nepal Himalaya. In: Advances in Geophysics, Dmowska, R. (Ed.), Elsevier, 2003.

Ayoub, F., Leprince, S., and Avouac, J. P.: Users Guide to COSI-CORR Co-registration of Optically Sensed Images and Correlation, http://www.tectonics.caltech.edu/slip_history/spot_coseis/pdf_files/CosiCorr-Guide2015a.pdf, 2015. 2015.

Blöthe, J. H., Korup, O., and Schwanghart, W.: Large landslides lie low: Excess topography in the Himalaya-Karakoram ranges, Geology, 43, 523-526, 2015.

Burbank, D. W., Leland, J., Fielding, E., Anderson, R. S., Brozovic, N., Reid, M. R., and Duncan, C.: Bedrock incision, rock uplift and threshold hillslopes in the northwestern Himalayas, Nature, 379, 505-510, 1996.

Chen, R.-F., Chang, K.-J., Angelier, J., Chan, Y.-C., Deffontaines, B., Lee, C.-T., and Lin, M.-L.: Topographical changes revealed by high-resolution airborne LiDAR data: The 1999 Tsaoling landslide induced by the Chi–Chi earthquake, Engineering Geology, 88, 160-172, 2006.

Chigira, M. and Yagi, H.: Geological and geomorphological characteristics of landslides triggered by the 2004 Mid Niigta prefecture earthquake in Japan, Engineering Geology, 82, 202-221, 2006.

Cowgill, E., Bernardin, T. S., Oskin, M. E., Bowles, C., Yıkılmaz, M. B., Kreylos, O., Elliott, A. J., Bishop, S., Gold, R. D., Morelan, A., Bawden, G. W., Hamann, B., and Kellogg, L. H.: Interactive terrain visualization enables virtual field work during rapid scientific response to the 2010 Haiti earthquake, Geosphere, 8, 787-804, 2012.

Dadson, S. J., Hovius, N., Chen, H., Dade, W. B., Hsieh, M.-L., Willett, S. D., Hu, J.-C., Horng, M.-J., Chen, M.-C., Stark, C. P., Lague, D., and Lin, J.-C.: Links between erosion, runoff variability and seismicity in the Taiwan orogen, Nature, 426, 648-651, 2003.

Dai, F. C. and Lee, C. F.: Landslide characteristics and slope instability modeling using GIS, Lantau Island, Hong Kong, Geomorphology, 42, 213-228, 2002.

Densmore, A. L., Ellis, M. A., and Anderson, R. S.: Landsliding and the evolution of normal-fault-bounded mountains, Journal of Geophysical Research: Solid Earth, 103, 15203-15219, 1998.

Dou, J., Paudel, U., Oguchi, T., Uchiyama, S., and Hayakawa, Y.: Shallow and Deep-Seated Landslide

Differentiation Using Support Vector Machines: A Case Study of the Chuetsu Area, Japan, Terrestial, Atmospheric and Oceanic Sciences, 26, 227-239, 2015.
Godard, V., Lavé, J., Carcaillet, J., Cattin, R., Bourlès, D., and Zhu, J.: Spatial distribution of denudation in Eastern Tibet and regressive erosion of plateau margins, Tectonophysics, 491, 253-274, 2010.
GSI: 2 m grid elevation data. Institute, G. S. (Ed.), 2007.
Hirata, N., Sato, H., Sakai, S. i., Kato, A., and Kurashimo, E.: Fault system of the 2004 Mid Niigata Prefecture Earthquake and its aftershocks, Landslides, 2, 153-157, 2005.
Hollingsworth, J., Leprince, S., Ayoub, F., and Avouac, J.-P.: Deformation during the 1975–1984 Krafla rifting crisis, NE Iceland, measured from historical optical imagery, Journal of Geophysical Research: Solid Earth, 117, B11407, , 2012.
Hovius, N., Meunier, P., Lin, C.-W., Chen, H., Chen, Y.-G., Dadson, S., Horng, M.-J., and Lines, M.: Prolonged seismically induced erosion and the mass balance of a large earthquake, Earth and Planetary Science Letters, 304, 347-355, 2011.
Hovius, N., Stark, C. P., and Allen, P. A.: Sediment flux from a mountain belt derived by landslide mapping, Geology, 25, 231-234, 1997.
Kato, A., Kurashimo, E., Hirata, N., Sakai, S., Iwasaki, T., and Kanazawa, T.: Imaging the source region of the 2004 mid-Niigata prefecture earthquake and the evolution of a seismogenic thrust-related fold, Geophysical Research Letters, 32, L07307,, 2005.
Kato, A., Sakai, S. i., Hirata, N., Kurashimo, E., Iidaka, T., Iwasaki, T., and Kanazawa, T.: Imaging the seismic structure and stress field in the source region of the 2004 mid-Niigata prefecture earthquake: Structural zones of weakness and seismogenic stress concentration by ductile flow, Journal of Geophysical Research: Solid Earth, 111, B08308, , 2006.
Kirby, E., Reiners, P. W., Krol, M. A., Whipple, K. X., Hodges, K. V., Farley, K. A., Tang, W., and Chen, Z.: Late Cenozoic evolution of the eastern margin of the Tibetan Plateau: Inferences from 40Ar/39Ar and (U-Th)/He thermochronology, Tectonics, 21, 1-1-1-20, 2002.
Lane, S. N., Chandler, J. H., and Porfiri, K.: Monitoring River Channel and Flume Surfaces with Digital Photogrammetry, Journal of Hydraulic Engineering, 127, 871-877, 2001.
Larsen, I. J. and Montgomery, D. R.: Landslide erosion coupled to tectonics and river incision, Nature Geoscience, 5, 468-473, 2012.
Leprince, S., Barbot, S., Ayoub, F., and Avouac, J. P.: Automatic and Precise Orthorectification, Coregistration, and Subpixel Correlation of Satellite Images, Application to Ground Deformation Measurements, Geoscience and Remote Sensing, IEEE Transactions on, 45, 1529-1558, 2007.
Li, G., West, A. J., Densmore, A. L., Jin, Z., Parker, R. N., and Hilton, R. G.: Seismic mountain building: Landslides associated with the 2008 Wenchuan earthquake in the context of a generalized model

for earthquake volume balance, Geochemistry, Geophysics, Geosystems, 15, 833-844, 2014.

Marc, O., Hovius, N., Meunier, P., Uchida, T., and Hayashi, S.: Transient changes of landslide rates after earthquakes, Geology, 43, 883-886, 2015.

Maruyama, T., Fusejima, Y., Yoshioka, T., Awata, Y., and Matsu'ura, T.: Characteristics of the surface rupture associated with the 2004 Mid Niigata Prefecture earthquake, central Japan and their seismotectonic implications, Earth Planet Sp, 57, 521-526, 2005.

Maruyama, T., Iemura, K., Azuma, T., Yoshioka, T., Sato, M., and Miyawaki, R.: Paleoseismological evidence for non-characteristic behavior of surface rupture associated with the 2004 Mid-Niigata Prefecture earthquake, central Japan, Tectonophysics, 429, 45-60, 2007.

McPhillips, D., Bierman, P. R., and Rood, D. H.: Millennial-scale record of landslides in the Andes consistent with earthquake trigger, Nature Geoscience, 7, 925-930, 2014.

Morell, K. D., Sandiford, M., Rajendran, C. P., Rajendran, K., Alimanovic, A., Fink, D., and Sanwal, J.: Geomorphology reveals active décollement geometry in the central Himalayan seismic gap, Lithosphere, 7, 247-256, 2015.

Nakata, T. and Imaizumi, T.: Digital Active Fault map of Japan, University of Tokyo Press, Tokyo, 2002.

Nissen, E., Maruyama, T., Ramon Arrowsmith, J., Elliott, J. R., Krishnan, A. K., Oskin, M. E., and Saripalli, S.: Coseismic fault zone deformation revealed with differential lidar: Examples from Japanese ~7 intraplate earthquakes, Earth and Planetary Science Letters, 405, 244-256, 2014.

Okamura, Y.: Fault-related folds and an imbricate thrust system on the northwestern margin of the northern Fossa Magna region, central Japan, Island Arc, 12, 61-73, 2003.

Okamura, Y., Ishiyama, T., and Yanagisawa, Y.: Fault-related folds above the source fault of the 2004 mid-Niigata Prefecture earthquake, in a fold-and-thrust belt caused by basin inversion along the eastern margin of the Japan Sea, Journal of Geophysical Research: Solid Earth, 112, B03S08, , 2007.

Okamura, Y., Watanabe, M., Morijiri, R., and Satoh, M.: Rifting and basin inversion in the eastern margin of the Japan Sea, Island Arc, 4, 166-181, 1995.

Ouimet, W. B.: Landslides associated with the May 12, 2008 Wenchuan earthquake: Implications for the erosion and tectonic evolution of the Longmen Shan, Tectonophysics, 491, 244-252, 2010.

Owen, L. A.: Landscape development of the Himalayan–Tibetan orogen: a review, Geological Society, London, Special Publications, 338, 389-407, 2010.

Ozawa, T., Nishimura, S., Wada, Y., and Ohkura, H.: Coseismic deformation of the Mid Niigata prefecture Earthquake in 2004 detected by RADARSAT/InSAR, Earth Planet Sp, 57, 423-428, 2005.

Parker, R. N., Densmore, A. L., Rosser, N. J., de Michele, M., Li, Y., Huang, R., Whadcoat, S., and Petley, D. N.: Mass wasting triggered by the 2008 Wenchuan earthquake is greater than orogenic growth, Nature Geoscience, 4, 449-452, 2011.

Solid Earth Discuss., https://doi.org/10.5194/se-2019-3
Manuscript under review for journal Solid Earth
Discussion started: 14 January 2019

Solid Earth
Discussions

Ren, Z. and Lin, A.: Co-seismic landslides induced by the 2008 Wenchuan magnitude 8.0 Earthquake, as revealed by ALOS PRISM and AVNIR2 imagery data, International Journal of Remote Sensing, 31, 3479-3493, 2010.

Ren, Z., Zhang, Z., Dai, F., Yin, J., and Zhang, H.: Topographic changes due to the 2008 Mw 7.9 Wenchuan earthquake as revealed by the differential DEM method, Geomorphology, 217, 122-130, 2014a.

Ren, Z., Zhang, Z., Dai, F., Yin, J., and Zhang, H.: Topographic changes due to the 2008 Mw 7.9 Wenchuan earthquake as revealed by the differential DEM method, Geomorphology, 217, 122-130, 2014b.

Ren, Z., Zhang, Z., and Yin, J.: Erosion Associated with Seismically-Induced Landslides in the Middle Longmen Shan Region, Eastern Tibetan Plateau, China, Remote Sensing, 9, 864, 2017.

RGAFJ: Active Faults in Japan:Sheet Maps and Inventories (revised edition), University of Tokyo Press, Tokyo, 1991.

Roering, J.: Tectonic geomorphology: Landslides limit mountain relief, Nature Geoscience, 5, 446-447, 2012.

Sato, H., Sekiguchi, T., Kojiroi, R., Suzuki, Y., and Iida, M.: Overlaying landslides distribution on the earthquake source, geological and topographical data: the Mid Niigata prefecture earthquake in 2004, Japan, Landslides, 2, 143-152, 2005.

Stumpf, A., Malet, J. P., Allemand, P., and Ulrich, P.: Surface reconstruction and landslide displacement measurements with Pléiades satellite images, ISPRS Journal of Photogrammetry and Remote Sensing, 95, 1-12, 2014.

Suppe, J.: Geometry and kinematics of fault-bend folding, American Journal of Science, 283, 684-721, 1983.

Wang, E., Kirby, E., Furlong, K. P., van Soest, M., Xu, G., Shi, X., Kamp, P. J. J., and Hodges, K. V.: Two-phase growth of high topography in eastern Tibet during the Cenozoic, Nature Geoscience, 5, 640-645, 2012.

Wang, H. B., Sassa, K., and Xu, W. Y.: Analysis of a spatial distribution of landslides triggered by the 2004 Chuetsu earthquakes of Niigata Prefecture, Japan, Nat Hazards, 41, 43-60, 2007.

Wei, D. and Seno, T.: Determination of the Amurian Plate Motion. In: Mantle Dynamics and Plate Interactions in East Asia, Flower, M. F. J., Chung, S. L., Lo, C. H., and Lee, C. F. (Eds.), American Geophysical Union, Washington, 1998.

Wheaton, J. M., Brasington, J., Darby, S. E., and Sear, D. A.: Accounting for uncertainty in DEMs from repeat topographic surveys: improved sediment budgets, Earth Surface Processes and Landforms, 35, 136-156, 2010.

Zhou, Y., Elliott, J. R., Parsons, B., and Walker, R. T.: The 2013 Balochistan earthquake: An

Solid Earth Discuss., https://doi.org/10.5194/se-2019-3
Manuscript under review for journal Solid Earth
Discussion started: 14 January 2019

extraordinary or completely ordinary event?, Geophysical Research Letters, 42, 6236-6243, 2015.

Zielke, O., Arrowsmith, J. R., Ludwig, L. G., and Akçiz, S. O.: Slip in the 1857 and Earlier Large Earthquakes Along the Carrizo Plain, San Andreas Fault, Science, 327, 1119-1122, 2010.

Captions to figures

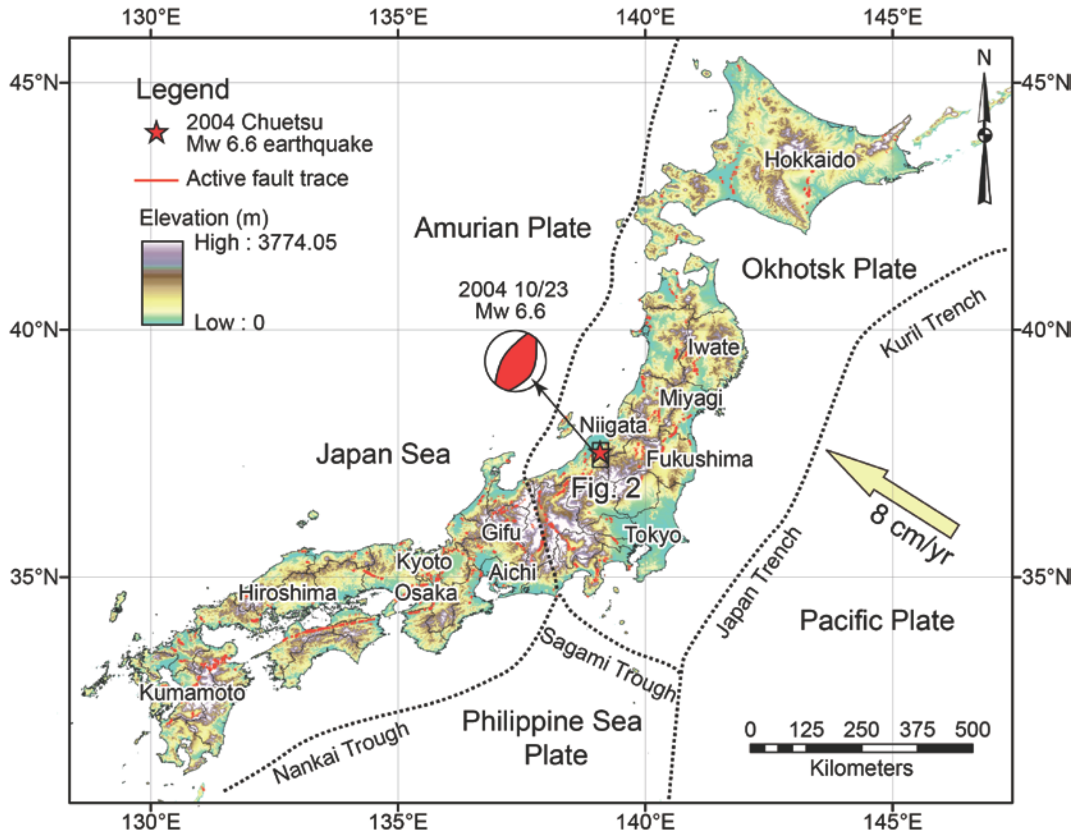

Figure 1. Plate tectonic framework and active faults in Japan. Active fault traces are from [RGFAFJ 1991; Nakata and Imaizumi, 2002]. The focal mechanism of the 2004 Mw 6.6 Chuetsu earthquake is from the Harvard Centroid Moment Tensor (CMT) catalog (http://www.globalcmt.org/CMTsearch.html). The red star indicates the epicenter of the 2004 Chuetsu earthquake. Black rectangle shows the detail location of Figure 2.

Solid Earth Discuss., https://doi.org/10.5194/se-2019-3
Manuscript under review for journal Solid Earth
Discussion started: 14 January 2019

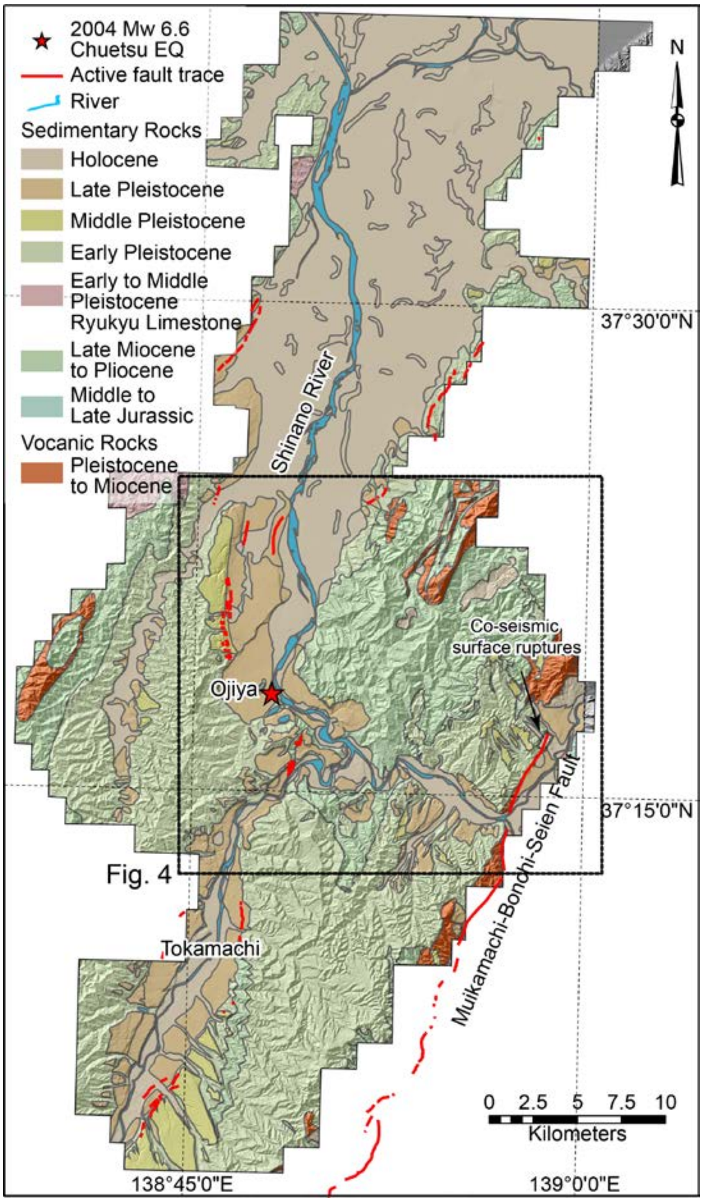

Figure 2. Geological map of the epicentral area of the 2004 Chuetsu earthquake. The red lines show the major active faults. The small rectangle shows the location of the co-seismic surface rupture of the 2004 Chuetsu earthquake, which occurred on the northward extending of the Muikamachi fault zone (Maruyama et al., 2005).

Solid Earth Discuss., https://doi.org/10.5194/se-2019-3
Manuscript under review for journal Solid Earth
Discussion started: 14 January 2019

Solid Earth
Discussions
Open Access

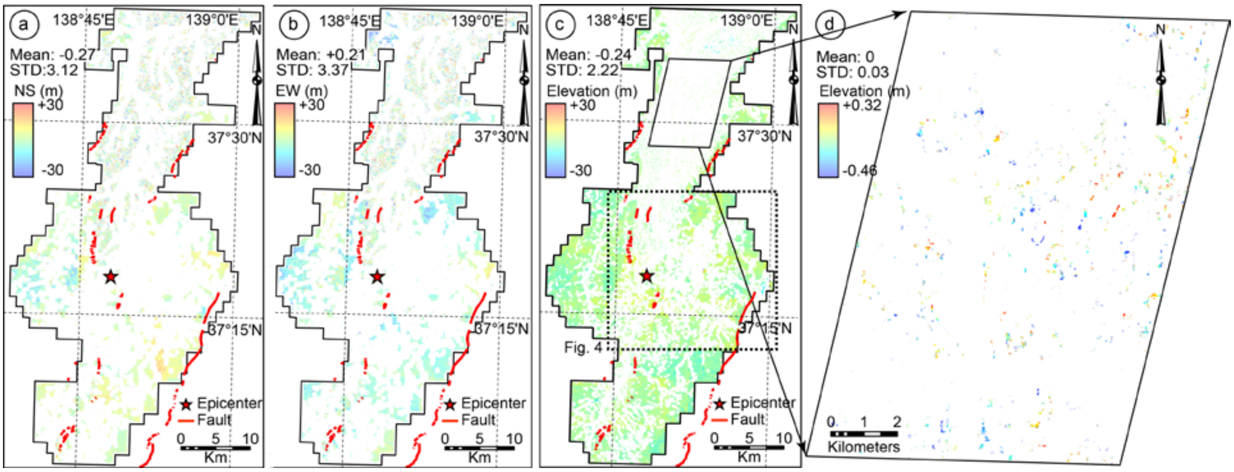

Figure 3. The horizontal differences between pre- and post-earthquake DEMs at NS direction (a), EW direction (b), the vertical deformations obtained by subtracting the pre-earthquake DEM from the post-earthquake DEM. (c), and the vertical deformations at the flat region far from the epicentral area (d). The flat region far from the epicentral area should be of no vertical deformation, which represents the accuracy of the differential DEM in this study. The dashed rectangle shows the location of Figure 4. The mean vertical deformation of the whole region is -0.24 m with standard deviation (STD) of 2.22 m. The white background indicates value of zero. The color scale is shown in min-max.

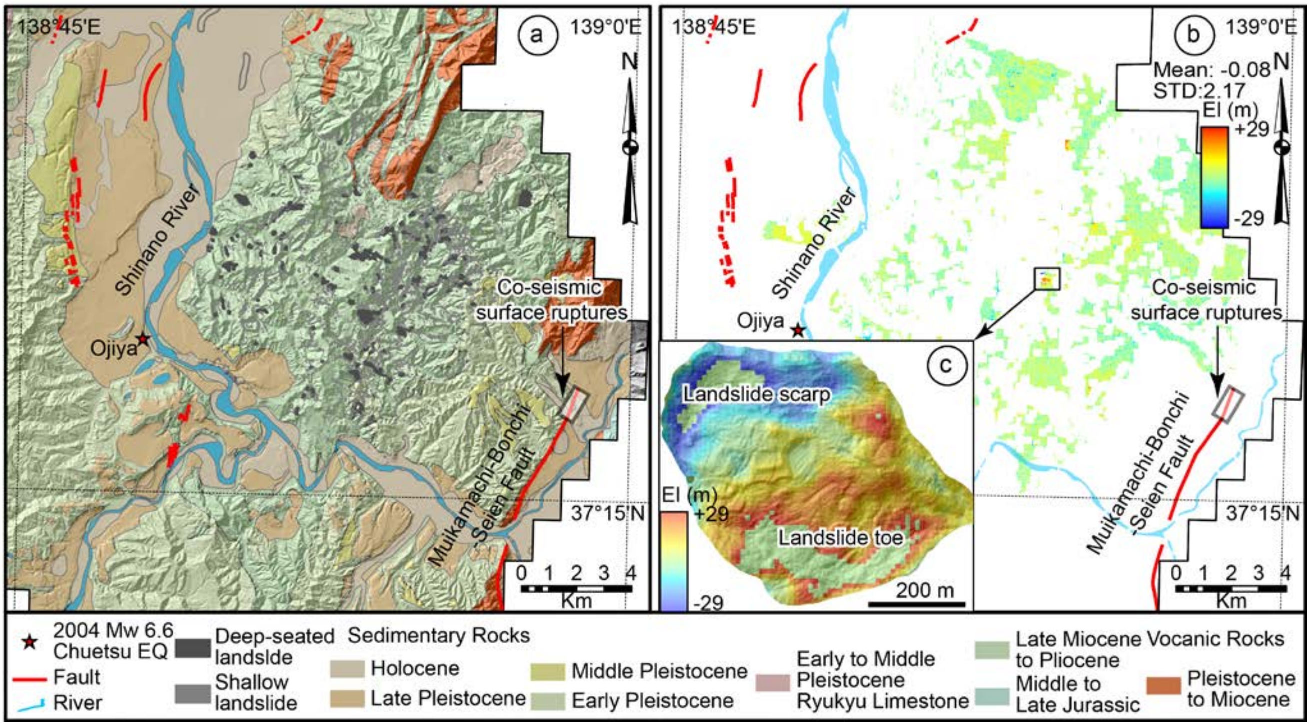

Figure 4. The geological map and distribution of co-seismic landslides (a) and vertical deformations at the epicentral area (b), the inset map shows the largest co-seismic landslide (c). The dark gray polygons show the deep-seated landslides and the light gray polygons show the shallow landslides. The landslide inventory map is from the National Research Institute for Earth Science and Disaster Prevention (NIED), Japan. The mean vertical deformation of the landslide region is -0.08 m with STD of 2.17 m. The white background indicates value of zero. The color scale is shown in min-max.

Solid Earth Discuss., https://doi.org/10.5194/se-2019-3
Manuscript under review for journal Solid Earth
Discussion started: 14 January 2019

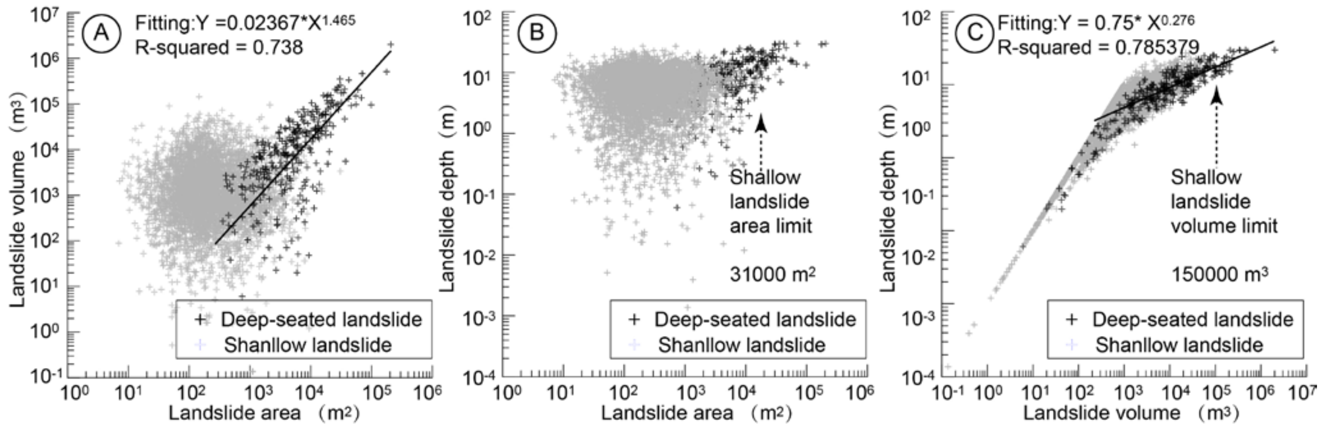

Figure 5. The relationship of landslide volume, landslide area and landslide depth. Landslide area and volume (a), Landslide depth and area (b), Landslide depth and landslide volume (c) obtained from pre- and post-earthquake DEMs.

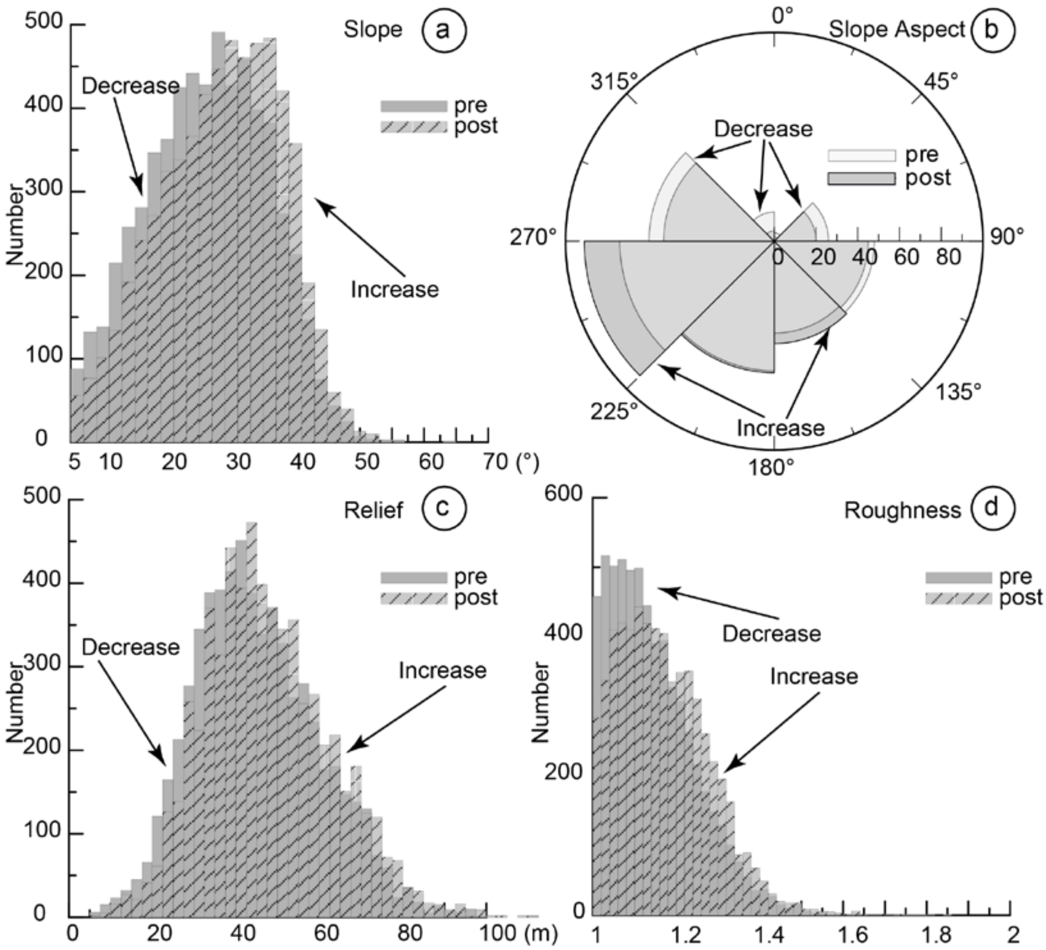

Figure 6. Statistical comparison of the pre- and post- earthquake slope angle (a), slope aspect (b), relief (c) and roughness (d).

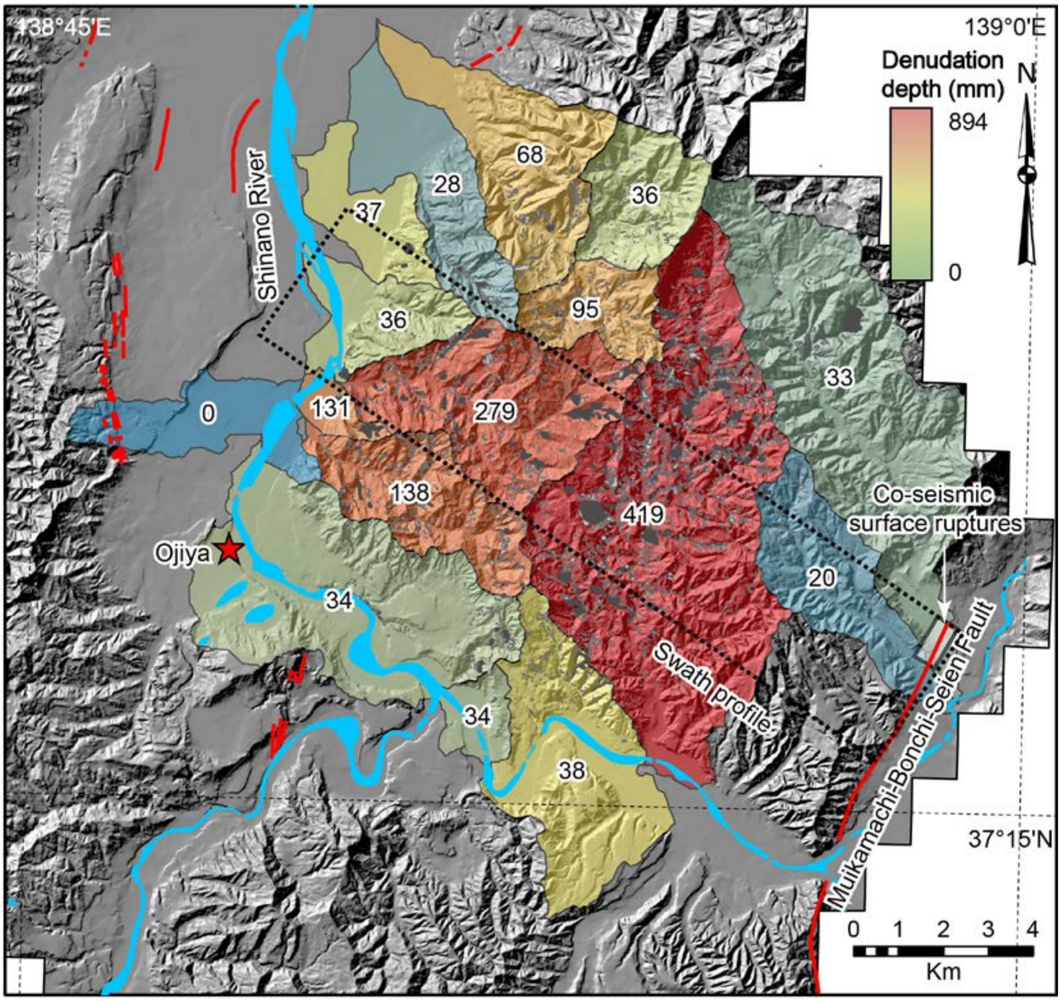

492

493 Figure 7. The distribution of catchment-scale average denudation. The denudation depths are obtained

494 by averaging the total landslide volume by the catchment area within each catchment.

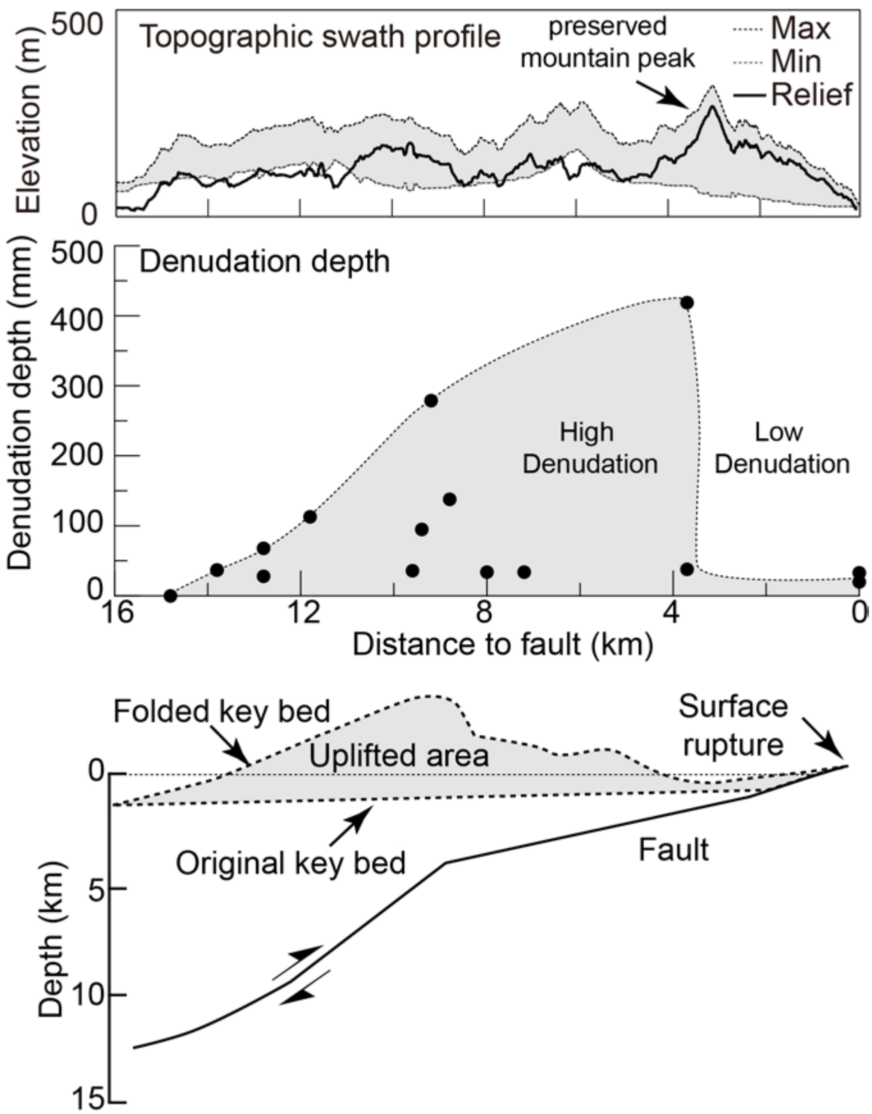

Figure 8. The topography swath profile, denudation depth and deformation pattern associated with fault-related folding of the Muikamachi fault. The deformation pattern was modified from (Kato et al., 2005; Kato et al., 2006; Okamura et al., 2007).